

Prognostic Insights from Longitudinal Multicompartment Study of Host-Microbiota Interactions in Critically Ill Patients.

Georgios Kitsios (✉ kitsiosg@upmc.edu)

University of Pittsburgh <https://orcid.org/0000-0002-1018-948X>

Khaled Sayed

University of Florida

Adam Fitch

University of Pittsburgh

Haopu Yang

Tsinghua University

Noel Britton

Johns Hopkins University

Faraaz Shah

University of Pittsburgh

William Bain

University of Pittsburgh <https://orcid.org/0000-0001-8506-0552>

John Evankovich

University of Pittsburgh

Shulin Qin

University of Pittsburgh

Xiaohong Wang

University of Pittsburgh

Kelvin Li

University of Pittsburgh Medical Center

Asha Patel

University of Pittsburgh

Yingze Zhang

University of Pittsburgh

Josiah Radder

University of Pittsburgh

Charles Dela Cruz

University of Pittsburgh

Daniel Okin

Massachusetts General Hospital

Ching-Ying Huang

Massachusetts General Hospital

Daria Van Tyne

University of Pittsburgh School of Medicine <https://orcid.org/0000-0001-7284-0103>

Panayiotis Benos

University of Florida

Barbara Methe

University of Pittsburgh

Peggy Lai

Massachusetts General Hospital

Alison Morris

University of Pittsburgh

Bryan McVerry

University of Pittsburgh <https://orcid.org/0000-0002-1175-4874>

Article

Keywords: microbiome, critical illness, dysbiosis, precision medicine, biomarkers

Posted Date: September 26th, 2023

DOI: <https://doi.org/10.21203/rs.3.rs-3338762/v1>

License:  This work is licensed under a Creative Commons Attribution 4.0 International License.

[Read Full License](#)

Additional Declarations: **Yes** there is potential Competing Interest. Dr. Kitsios has received research funding from Karius, Inc and Pfizer, Inc, both unrelated to this project. Dr. Morris has received research funding from Pfizer, Inc, unrelated to this project. Dr McVerry has received consulting fees from Boehringer Ingelheim, BioAegis, and Synairgen Research, Ltd. unrelated to this work. All other authors disclosed no conflict of interest.

1 **Prognostic Insights from Longitudinal Multicompartment Study of Host-Microbiota Interactions in**
2 **Critically Ill Patients.**

3
4 Georgios D. Kitsios, MD, PhD^{1,2*}; Khaled Sayed, PhD^{3,4}; Adam Fitch, MS²; Haopu Yang MDc⁵; Noel Britton,
5 PhD⁶; Faraaz Shah, MD, MPH^{1,7}; William Bain, MD^{1,7}; John W. Evankovich, MD;¹ Shulin Qin, MD, PhD^{1,2};
6 Xiaohong Wang, MS^{1,2}; Kelvin Li, MS²; Asha Patel, BS^{1,2}; Yingze Zhang, PhD¹; Josiah Radder, MD, PhD^{1,2},
7 Charles Dela Cruz, MD, PhD¹; Daniel A Okin, MD PhD⁸; Ching-Ying Huang, MS⁸; Daria van Tyne, PhD⁹;
8 Panayiotis V. Benos, PhD³; Barbara Methé, PhD^{1,2}; Peggy Lai, MD⁸; Alison Morris, MD, MS^{1,2^}; Bryan J.
9 McVerry, MD^{1,2^}

10
11 *Corresponding author

12 ^Co-senior authors

13
14 **Institutions/affiliations:**

15 1 - Division of Pulmonary, Allergy, Critical Care and Sleep Medicine, University of Pittsburgh, Pittsburgh, PA,
16 USA

17 2 - Center for Medicine and the Microbiome, University of Pittsburgh, Pittsburgh, PA, USA

18 3 - Department of Epidemiology, University of Florida, Gainesville, FL, USA.

19 4 - Department of Electrical and Computer Engineering & Computer Science, University of New Haven, West
20 Haven, CT, USA

21 5- School of Medicine, Tsinghua University, Beijing, China

22 6- Division of Pulmonary Critical Care Medicine, Department of Medicine, Johns Hopkins University School of
23 Medicine, Baltimore, Maryland, USA

24 7- Veteran's Affairs Pittsburgh Healthcare System, Pittsburgh, PA, USA.

25 8- Division of Pulmonary and Critical Care Medicine, Massachusetts General Hospital and Harvard Medical
26 School, Boston, MA, USA

27 9- Division of Infectious Diseases, Department of Medicine, University of Pittsburgh, Pittsburgh, PA, USA

28

29

30 Corresponding author:

31 Georgios D. Kitsios, MD, PhD

32 Assistant Professor of Medicine

33 Division of Pulmonary, Allergy, Critical Care and Sleep Medicine

34 University of Pittsburgh Medical Center

35 Address: UPMC Montefiore Hospital, NW628, 3459 Fifth Avenue, Pittsburgh, PA 15213

36 Email: kitsiosg@upmc.edu

37

38

39 **Author's contributions:**

40 **Author A:** Conceptualization, Methodology, Validation, Investigation, Resources, Writing - Original Draft,
41 Writing - Review & Editing, Visualization, Project administration; **Georgios D. Kitsios:** Conceptualization,
42 Methodology, Validation, Formal analysis, Investigation, Resources, Writing - Original Draft, Writing - Review &
43 Editing, Visualization, Supervision, Project administration, Funding acquisition; **Authors B, C, D:** Investigation,
44 Writing - Review & Editing

45

46 **Conflicts of Interest:** Dr. Kitsios has received research funding from Karius, Inc and Pfizer, Inc, both
47 unrelated to this project. Dr. Morris has received research funding from Pfizer, Inc, unrelated to this project. Dr
48 McVerry has received consulting fees from Boehringer Ingelheim, BioAegis, and Synairgen Research, Ltd.
49 unrelated to this work. All other authors disclosed no conflict of interest.

50 **Funding information:** Dr. Kitsios: University of Pittsburgh Clinical and Translational Science Institute, COVID-
51 19 Pilot Award; NIH (R03 HL162655); Dr. Benos: NIH (R01 HL157879; R01 HL127349, R01DK130294); Dr.
52 McVerry: NIH (P01 HL114453); Dr. Bain: Veterans Affairs (IK2BX004886); Dr. Lai: Massachusetts General
53 Hospital Translational and Clinical Research Center, supported by Grant 1UL1TR002541

54

55

56 **Abstract**

57 Critical illness can disrupt the composition and function of the microbiome, yet comprehensive longitudinal
58 studies are lacking. We conducted a longitudinal analysis of oral, lung, and gut microbiota in a large cohort of
59 479 mechanically ventilated patients with acute respiratory failure. Progressive dysbiosis emerged in all three
60 body compartments, characterized by reduced alpha diversity, depletion of obligate anaerobe bacteria, and
61 pathogen enrichment. Clinical variables, including chronic obstructive pulmonary disease, immunosuppression,
62 and antibiotic exposure, shaped dysbiosis. Notably, of the three body compartments, unsupervised clusters of
63 lung microbiota diversity and composition independently predicted survival, transcending clinical predictors,
64 organ dysfunction severity, and host-response sub-phenotypes. These independent associations of lung
65 microbiota may serve as valuable biomarkers for prognostication and treatment decisions in critically ill
66 patients. Insights into the dynamics of the microbiome during critical illness highlight the potential for
67 microbiota-targeted interventions in precision medicine.

68

69

70

71 **Keywords:** microbiome, critical illness, dysbiosis, precision medicine, biomarkers

72 .

73 Introduction

74 Microbiota play a critical role in maintaining homeostasis and overall health. However, during critical
75 illness, such as acute respiratory failure (ARF), microbial communities can be severely disrupted.^{1,2} Such
76 disruptions, characterized by deviations from a healthy microbial composition and diversity, may occur early in
77 the hospital stay and have been associated with worse clinical outcomes.³⁻⁵ Previous research has primarily
78 focused on cross-sectional analyses of microbiota within individual body sites, neglecting potential interactions
79 between different compartments and the longitudinal evolution of microbial communities. Moreover, the
80 influence of patient-level factors and therapeutic interventions, including antimicrobial therapies, on the
81 microbiome of critically ill patients remains poorly understood, partly due to limitations of scale in studies
82 published to date.

83 Precision medicine approaches in ARF have predominantly focused on host factors.⁶ For instance,
84 identifying distinct subphenotypes based on patterns of host response biomarkers measured in plasma
85 samples (hyper- vs. hypo-inflammatory) has demonstrated prognostic value.⁷⁻⁹ Hyperinflammatory patients
86 exhibit elevated levels of injury and inflammation biomarkers, more severe organ dysfunction, worse prognosis,
87 and may have distinct responses to treatments.⁸ However, the role of respiratory or intestinal microbiota in
88 modulating host responses and their contributions to defined subphenotypes are still not well understood.
89 Furthermore, limited data are available regarding the potential influence of respiratory microbiota on systemic
90 host responses measured in plasma or localized inflammation within the lungs.¹⁰ To advance precision
91 medicine approaches that take into account the microbial side of the critically ill host, it is crucial to understand
92 the dynamics of the microbiome and its relationship with host biological factors, clinical diagnoses, and
93 therapeutic interventions in critical illness.

94 To address these knowledge gaps, we conducted a longitudinal assessment of the microbiome in a
95 large cohort of 479 ARF patients, specifically focusing on three key body sites: the oral cavity, lungs, and gut.
96 By integrating bacterial and fungal community profiles with host response biomarkers measured in plasma and
97 lower respiratory tract (LRT) samples, we examined the temporal associations between patient-level factors
98 and therapeutic interventions on microbial communities. We derived unsupervised clusters of microbiota and

determined their associations with host-response subphenotypes and clinical outcomes. Finally, we validated our findings in two separate cohorts with a total of 146 patients with COVID-19-associated ARF.

Results

Cohort Description:

We performed discovery analyses in a cohort of 479 patients with ARF who received invasive mechanical ventilation (IMV) via endotracheal intubation in UPMC Intensive Care Units (ICUs) (**UPMC-ARF cohort**), and then independent validation analyses in two cohorts of critically ill patients with COVID-19 pneumonia (49 patients at UPMC [**UPMC-COVID cohort**], and 97 patients at Massachusetts General Hospital ICUs, **MGH-COVID cohort**).

In the UPMC-ARF cohort, we enrolled patients with non-COVID etiologies of ARF between March 2015 and June 2022. We collected baseline research biospecimens within 72hrs from intubation, including blood for separation of plasma, oropharyngeal swabs (oral samples), endotracheal aspirates (ETA) collected for research or excess bronchoalveolar lavage fluid (BALF) from clinical bronchoscopy (lung samples), and rectal swabs or stool (gut samples).^{3,11,12} We repeated research biospecimen sampling between days 3-6 (middle interval) and days 7-12 (late interval) post-enrollment for subjects who remained in the ICU. We extracted DNA and performed next-generation sequencing (bacterial 16S rRNA gene sequencing [16S-Seq] for all available samples; fungal Internal Transcribed Spacer sequencing [ITS-Seq] targeting the regions 1 and 2 of the ITS rRNA gene, and Nanopore DNA metagenomics for a subset of samples) to profile microbiota in the oral, lung and gut communities, respectively.^{3,12,13} We measured biomarker proteins in plasma samples and ETA/BALF supernatants with Luminex panels to profile systemic and regional (lung) host responses.^{7,10}

Patients had a median (interquartile range) age of 59.6 (46.7-68.7) years, 54.4% were men and 90.2% were whites (Table 1). At the time of enrollment, 25.0% of patients were diagnosed with Acute Respiratory Distress Syndrome (ARDS per the Berlin definition¹⁴) and 39.8% with pneumonia, 86.8% were receiving systemic antibiotics, and 64.8% received corticosteroids for various indications. By 60 days, 26.9% of patients had died. Among the 350 patients who survived hospitalization, 48.8% were discharged to their home, with the remainder requiring additional longer-term care.

125 In the UPMC-COVID cohort, we enrolled 49 patients with COVID-19 ARDS requiring IMV and obtained
126 longitudinal plasma and ETA samples at baseline, middle and late intervals (Table S1). We performed 16S
127 sequencing for bacteria and measured host response biomarkers in both sample types. In the MGH-COVID
128 cohort, we enrolled 97 hospitalized patients, obtained serial lung (sputum or ETA) and stool (gut) samples
129 (Table S1) and performed Illumina metagenomics.¹⁵ To contextualize microbiota analyses from critically ill
130 patients, we incorporated previously generated 16S-Seq data from upper respiratory tract (URT), LRT and
131 stool samples collected from healthy volunteers (**Healthy Controls**), as previously described in smaller cross-
132 sectional studies from our group.^{11,12}

134 Progressive dysbiosis of microbial communities in three body compartments.

135 Among all three cohorts and healthy controls, we analyzed a total of 2557 clinical samples and 233
136 experimental control samples, with the latter obtained either during patient sampling at the bedside or during
137 sample processing in the laboratory. In an initial quality control step, we demonstrated robust detection of
138 bacterial 16S reads in oral, lung and gut samples in the UPMC-ARF cohort compared to negative controls
139 (Figure S1A-B). We also found that rectal swabs not coated by stool (“unsoiled” swabs) had systematic
140 differences in bacterial load (16S rRNA gene copies by qPCR) and beta diversity (Manhattan distances)
141 compared to stool or visibly “soiled” rectal swabs (Figure S1C-D). Therefore, we excluded “unsoiled” rectal
142 swabs from further analyses because they may not offer sufficient representation of gut microbiota.¹¹

143 Samples from critically ill patients had significantly lower alpha diversity (Shannon index) in each
144 compartment compared to corresponding healthy control samples. Alpha diversity further declined in all three
145 body compartments across longitudinal samples (Figure 1A). Similarly, baseline ICU samples had markedly
146 significant differences in beta diversity from healthy controls (Figure 1B). Taxonomic composition comparisons
147 showed depletion of multiple commensal taxa in ICU samples, with significant enrichment for *Staphylococcus*
148 in oral and lung samples, and *Anaerococcus* and *Staphylococcus* in gut samples (Figure 1C-D-E). Among ICU
149 samples, bacterial load quantification by 16S qPCR confirmed that the LRT had significantly lower biomass
150 compared to URT (oral) and gastrointestinal tract (Figure 1F).

151 We then examined the compositional similarity (Bray-Curtis indices) between compartments to
152 understand the relationship between the low biomass (lung) vs. high biomass (oral and gut) communities. We
153 found higher similarity between oral-lung vs. gut-lung communities in the baseline and middle intervals (Figure
154 1G). Taxonomic comparisons between compartments revealed that no specific taxa were systematically
155 different between oral and lung microbiota (Figure 1H), whereas in gut-lung comparisons, lung communities
156 were enriched for typical respiratory commensals (e.g. *Rothia*, *Veillonella*, *Streptococcus*) and gut communities
157 for gut commensals (e.g. *Bacteroides*, *Lachnoclostridium*, *Lachnospiraceae_uncl*) (Figure 1I). We specifically
158 tested whether certain patients had enrichment for gut-origin bacteria in their oral or lung samples despite no
159 overall enrichment of the lung compartment for gut bacteria. We found that 4.8% and 8.1% of oral and lung
160 samples, respectively, had >30% relative abundance for gut-origin bacteria (Fisher's test $p=0.03$, Figure S2A),
161 with progressively increased enrichment over time (Fisher's test = 0.02, Figure S2B) in lung samples.
162 Importantly, the gut-origin taxa enrichment in these lung samples could not be fully explained by oropharyngeal
163 colonization with such taxa (Figure S2C). Taken together, these multi-site analyses point to the oral cavity as
164 the primary source of lung microbiota, which could be seeded by micro-aspiration along the respiratory tract's
165 gravitational gradient. At the same time, our analyses also provided evidence for gut-origin bacteria enrichment
166 in the LRT in a subset of critically ill patients.

167 We next examined the longitudinal composition of microbial communities by classifying bacteria in
168 terms of their oxygen requirements (obligate anaerobes, facultative anaerobes, aerobes, microaerophiles,
169 variable or unclassifiable) and plausible respiratory pathogenicity (oral commensals, recognized respiratory
170 pathogens or other).¹² In both oral and lung communities, we found a progressive decline in the relative
171 abundance of obligate anaerobes over time. There was, however, no corresponding change in the gut
172 composition of anaerobic (obligate or facultative) bacteria over time (Figure 2A-B). Stratified by plausible
173 pathogenicity, we found a progressive decline of oral commensal bacteria in all three compartments, with a
174 corresponding increase in pathogen abundance (Figure 2C-D). Fungal ITS sequencing showed that >50% of
175 communities in all three compartments were dominated by *C. albicans* (defined as >50% relative abundance),
176 with a progressive decline in fungal Shannon index in oral and lung communities during follow-up (Figure S3).
177 Nanopore metagenomics of lung samples provided similar bacterial representations to 16S analyses and

178 confirmed high abundance of *C.albicans* detected by ITS sequencing (Figure S3). Thus, our analyses revealed
179 a pattern of compartment-wide dysbiosis in ICU patients, with progressive decline in diversity and enrichment
180 for plausible pathogenic bacteria and *C. albicans*. We then sought to understand whether patient-level
181 variables accounted for baseline or longitudinal dysbiosis.

183 Clinical diagnoses and antibiotic exposure correlate with microbial community diversity and composition.

184 We constructed linear regression models with ecological metrics indicative of dysbiosis as outcomes
185 (baseline Shannon index, obligate anaerobe and respiratory pathogen abundance) and clinical variables as
186 predictors (Figure S4). History of COPD, immunosuppression and clinical diagnosis of pneumonia showed the
187 most significant associations with dysbiosis features, e.g. lower Shannon and anaerobe abundance in oral and
188 lung communities for patients with COPD, and increased pathogen abundance in all three compartments for
189 patients with history of immunosuppression (Figure S4). History of immunosuppression was also associated
190 with higher abundance of *C. albicans* in oral and lung samples (Figure S3D). To further explore iatrogenic
191 forces on microbiota composition, we focused on two common treatments in the ICU: antibiotics and steroids.
192 We assessed antibiotic usage by i) anaerobic coverage, ii) a numerical scale that included duration, timing and
193 type,¹⁶ and iii) the Narrow Antibiotic Treatment (NAT) score.^{12,17} We quantified steroid use as the daily
194 equivalent dosage of prednisone in milligrams. Antibiotic usage was associated with Shannon index, anaerobe,
195 and pathogen abundance in baseline gut samples, with exposure to antibiotics with anaerobic spectrum at
196 baseline being inversely correlated with anaerobe abundance in all three compartments (Figure S4B). To
197 explore the effects of antibiotics and steroids over time, we employed mixed linear regression models using
198 longitudinal samples. In all three compartments, the receipt of anaerobic spectrum antibiotics was associated
199 with a progressive decrease in obligate anaerobe abundance, without significant effects on pathogen
200 abundance (Table S2). Notably, antibiotic exposure quantified by the NAT score was also significantly linked to
201 a reduction in anaerobe abundance and an increase in pathogen abundance within the gut microbiota.
202 Steroids were associated with decrease in anaerobes in the lungs, but not with changes in abundance of other
203 microbes in other compartments.

205 Microbial communities in each compartment form distinct clusters of diversity and composition.

206 We next examined the microbial communities independent of clinical variables to capture important
207 features directly from microbiome data. To understand microbial heterogeneity within compartments, we
208 leveraged two complementary unsupervised clustering approaches: i) Dirichlet Multinomial Mixture (DMM)
209 models for 16S data in each compartment (“bacterial DMM clusters”) and for Nanopore metagenomic data in
210 the lung compartment¹⁸, and ii) weighted Similarity Network Fusion (SNF)¹⁹ clusters for combined bacterial
211 (16S) and fungal (ITS) data within each compartment (“bacterial-fungal SNF clusters”).

212 By bacterial DMM clusters, a three-class model offered optimal classification in each compartment, with
213 striking differences in alpha diversity and composition between clusters (Figure 3A). Cluster 1 in each
214 compartment had high Shannon index in the range of healthy controls (referred to as High-Diversity cluster),
215 cluster 3 had low Shannon index (Low-Diversity cluster), and cluster 2 had intermediate diversity (Intermediate-
216 Diversity cluster). Low-diversity clusters had markedly higher abundance of pathogens and lower abundance of
217 anaerobes (Figure 3B-C). In cross-compartment comparisons, DMM cluster membership was strongly
218 associated between oral and lung communities (odds ratio of membership in the Low-Diversity cluster in both
219 compartments 9.74, 95% confidence interval [5.61-17.29], $p < 0.0001$), whereas lung and gut clusters were less
220 strongly associated although statistically significant ($p = 0.015$, Figure 3D). In longitudinal analyses, cluster
221 membership showed relative stability for all compartments, with most samples assigned to Low-Diversity
222 cluster at baseline being assigned to Low-Diversity in the middle interval as well (77% of oral, 80% of lung, and
223 78% of gut samples, respectively, Figure S5). Nanopore DMM clustering in 130 available lung samples also
224 showed optimal fit with three total clusters (data not shown). Bacterial-Fungal SNF clustering revealed distinct
225 communities in each compartment, with a notable cluster in lung samples (cluster 1) with high pathogen
226 abundance and *C. albicans* dominance (near 100% of fungal sequences abundance) (Figure S6). Thus, our
227 unsupervised clustering approaches captured broad differences in meta-communities that were not specific to
228 individual taxa. We next examined how these microbial communities related to host responses and clinical
229 outcomes.

230
231 Lung microbiota correlate with systemic host responses.

232 We examined host-microbiota interactions with two independent approaches, a microbiota- and a host-
233 centric approach. In the microbiota-centric approach, we correlated the top 20 abundant taxa in each
234 compartment with systemic (plasma) and lung-specific (ETA/BALF supernatants) host response biomarkers.
235 We found several significant correlations (Figure S7A-C), with typical pathogens (e.g. *Klebsiella*, *Escherichia*-
236 *Shigella*, *Staphylococcus* genera in the lung compartment) positively correlating with plasma inflammatory
237 biomarkers (such as sTNFR1 and IL-6 levels), whereas typical oral commensals (e.g. *Rothia*, *Streptococcus*,
238 *Prevotella* etc.) inversely correlated with plasma sTNFR1 or sRAGE. In cluster comparisons, the bacterial
239 DMM Low-Diversity cluster in the lungs was significantly associated with higher plasma sTNFR1, sRAGE and
240 procalcitonin levels (Figure S7D), whereas the Nanopore DMM Low-Diversity cluster was also significantly
241 associated with higher regional (IL-6 and sRAGE) and systemic biomarkers of injury and inflammation (plasma
242 IL-6, sTNFR1, sRAGE, Ang-2 and Pentraxin-3, Figure S7E).

243 In the host-centric approach, we applied a widely validated framework of host-response subphenotypes
244 based on plasma biomarkers.^{7,20} With a validated 4-biomarker parsimonious model (using sTNFR1, Ang2,
245 procalcitonin and bicarbonate levels),²⁰ we classified individuals at baseline into a hyperinflammatory (22.9%)
246 vs. a hypoinflammatory (77.1%) subphenotype. We found no significant relationship between host
247 subphenotypes and DMM microbiota clusters in any compartment (Figure S7G), but hyperinflammatory
248 patients had higher pathogen abundance in lung communities ($p=0.04$). To further investigate this association,
249 we stratified patients by pneumonia diagnosis. We discovered that hyperinflammatory patients without
250 pneumonia had higher pathogen abundance in lung samples compared to hypo-inflammatory patients
251 ($p=0.018$, Figure S7H). These notable associations between lung pathogen abundance and the
252 hyperinflammatory subphenotype imply that systemic subphenotypes might stem, at least in part, from
253 undiagnosed pneumonia or respiratory dysbiosis.

254 Lung microbiota clusters predict survival independent of clinical variables and host responses.

256 Comparisons of microbial communities between survivors and non-survivors at 60-days post-ICU
257 admission showed highly significant differences in alpha diversity in the lungs ($p<0.0001$), as well as higher
258 obligate anaerobe and lower pathogen abundance in both oral and lung samples (all $p<0.002$, Figure S8A-C),

259 but no differences in gut profiles. Additionally, analyses of lung samples stratified by whether they exhibited
260 gut-origin taxa enrichment (defined as >30% relative abundance) showed markedly worse survival for patients
261 with gut-origin taxa enrichment ($p < 0.0001$, Figure S2E-F).

262 Analyses by bacterial DMM clusters provided further insights with regards to the prognostic value of
263 each compartment. In both oral and lung compartments, the Low-Diversity clusters were associated with worse
264 60-day survival in Kaplan-Meier curve analyses, whereas gut clusters had no survival impact (Figure 4A-C).
265 Notably, the prognostic effects of the Low-Diversity bacterial DMM cluster in the lungs remained significant
266 after adjustment for age, sex, history of COPD, immunosuppression, severity of illness by SOFA scores and
267 host-response subphenotypes (adjusted Hazards Ratio-HR= 2.51 [1.26-4.98], $p = 0.008$). Similarly, survival
268 analysis by the bacterial-fungal SNF lung clusters showed that cluster 1, which had high pathogen and *C.*
269 *albicans* abundance, also independently predicted worse survival (adjusted HR=2.04 [1.45-2.86], $p < 0.0001$,
270 Figure 4E). The other bacterial-fungal SNF oral and gut clusters did not impact survival (Figure 4D,F). Thus,
271 we found evidence that lung microbiota dysbiosis predicted survival beyond the information provided by clinical
272 predictors, commonly used organ dysfunction indices, and biological subphenotyping.

273 274 Derivation of a dysbiosis index and external validation in patients with COVID-19.

275 Motivated by the robust, independent prognostic impact of microbiota clusters on patient survival, we
276 next sought to construct predictive models to classify bacterial profiles into the corresponding DMM clusters
277 within each compartment. Such predictive models could serve as dysbiosis indices beyond the derivation
278 cohort with our DMM analysis. We used probabilistic graphical modeling (PGM) to predict the DMM clusters in
279 each compartment based on the abundance of the top 50 taxa and the corresponding Shannon index. By
280 splitting the dataset in training and testing subsets (80% and 20% of data points, respectively), we developed
281 separate multinomial regression models for DMM cluster predictions in each compartment (i.e. compartment-
282 specific Dysbiosis Index), which showed accuracy of 0.76, 0.86 and 0.75 for oral, lung and gut clusters,
283 respectively. We verified that patients classified in the low diversity clusters by the Dysbiosis Index for the oral
284 and lung compartments had worse survival, similarly to the DMM-derived clusters.

285 We next applied the derived Dysbiosis Indices to two independent cohorts of hospitalized patients with
286 COVID-19 pneumonia. In the UPMC-COVID cohort of patients with COVID-19 ARDS on IMV (n=49), the Lung
287 Dysbiosis Index classified ETA samples into three clusters with significant differences in Shannon index and
288 bacterial load by qPCR (Figure 5A), but no difference in ETA SARS-CoV-2 viral load by qPCR or 60-day
289 survival (data not shown). Patients assigned to the low diversity cluster at baseline had higher plasma levels of
290 sTNFR1 and Ang-2 compared to the high diversity cluster ($p < 0.05$, Figure 5B). By individual taxa abundance,
291 oral commensals (e.g. *Prevotella*, *Veillonella* or *Streptococcus*) were inversely correlated with plasma sTNFR1
292 and Ang-2, whereas *Klebsiella* abundance was positively correlated (all $p < 0.05$), corroborating the findings of
293 the cluster analyses relating lung microbiota with prognostically adverse higher levels of systemic biomarkers
294 of inflammation and endothelial injury.

295 In the MGH-COVID cohort (n=97), we performed metagenomic sequencing in longitudinal lung (ETA for
296 patients on IMV or expectorated sputum in spontaneously breathing patients) and gut (stool) samples obtained
297 upon enrollment and then daily up to day 4. We found no significant changes over time in Shannon Index and
298 anaerobe/pathogen abundance in either compartment on serial samples through day 4. We classified baseline
299 lung and gut samples by our Dysbiosis Index models, which showed significant differences in Shannon index,
300 anaerobe and pathogen abundance in each compartment (Figure 5C-D). Importantly, the low diversity cluster
301 in the lung compartment was strongly associated with COVID-19 pneumonia severity (odds ratio 8.77 [1.75-
302 67.74], Figure 5E-F), as classified by oxygen support requirements, whereas gut clusters were not. Thus,
303 application of the Dysbiosis Indices to lung and gut samples of patients with COVID-19 provided similar
304 findings to the ones obtained in the UPMC-ARF derivation cohort, supporting the predictive value of lung
305 microbiota profiling.

307 **Discussion:**

308 We conducted a longitudinal, integrative assessment of host-microbiota interactions in a large cohort of
309 ARF patients across three body sites (the oral cavity, lungs, and gut) and up to three time-points in the ICU.
310 These analyses offered insights into the temporal relationships between patient-level factors, therapeutic
311 interventions, microbial communities and patient-centered outcomes, which has not been possible in previous

312 smaller scale investigations.²¹ The progressive dysbiosis of microbial communities observed in all three body
313 compartments highlights the impact of critical illness on the global microbiota. We found reduced alpha
314 diversity and deviation in composition compared to healthy controls at the onset of IMV, with further reduction
315 in diversity and alterations in composition for patients supported on ventilators over time. Unsupervised
316 analyses of microbiota composition revealed distinct communities in all three body compartments, yet the lung
317 microbiome emerged as the strongest independent predictor of important clinical outcomes. We developed
318 parsimonious models for dysbiosis classifications in each compartment and found that lung dysbiosis was
319 significantly associated with host-response profiles and clinical severity in patients with COVID-19.

320 The large sample size and granular clinical data in our derivation cohort allowed for detailed
321 investigation of the relationships between patient-/treatment-related factors with the composition of microbiota.
322 Clinical diagnoses (e.g., ARDS or pneumonia) and comorbidities explained variation in diversity and
323 composition at baseline. We detected significant associations between systemic steroid exposure and lung
324 microbiota composition, a novel finding that warrants validation in other cohorts. Despite the self-evident
325 biological plausibility of antibiotic pressures on altering the microbiomes of critically ill patients, empirical
326 evidence to date has been limited.²²⁻²⁴ Here we modeled antibiotic exposure thoroughly with different
327 methodologies from prior studies focused on cystic fibrosis or pneumonia,^{16,17,25} and studied antibiotic effects
328 on longitudinal communities and features of dysbiosis. We found that the NAT score and a simple categorical
329 classification with regards to anaerobic spectrum coverage captured important effects on longitudinal
330 composition. Recent epidemiologic and molecular evidence supports disruptive effects of anti-anaerobic
331 antibiotics in gut microbial communities.^{24,26} Our data are consistent with the idea that anaerobe-targeting
332 antibiotics are associated with anaerobic bacteria depletion in the respiratory and the intestinal tracts, and
333 furthermore our study suggests that such depletion is associated with worse clinical outcome. Therefore, our
334 results highlight the importance of rational use of anti-anaerobic antibiotics as directed by proper clinical
335 indications, because such antibiotics can have important yet under-recognized adverse clinical implications.

336 The biogeography of the intubated respiratory tract has been the focus of extensive investigation for
337 prevention of secondary ventilator-associated pneumonia (VAP).^{27,28} Oropharyngeal decontamination with

338 chlorhexidine rinses or the more aggressive selective digestive decontamination (SDD) of the gastrointestinal
339 tract have been studied for reducing bacterial burden in probable source compartments that seed the LRT
340 microbiota. While both decontamination approaches are supported by randomized clinical trial evidence
341 showing efficacy in VAP prevention^{29,30}, both approaches also have associated safety concerns,^{31,32} leading to
342 limited uptake of SDD worldwide. Indiscriminate application of chlorhexidine rinses in all patients on IMV may
343 also deplete commensal organisms from the URT and reduce colonization resistance against pathogens. We
344 found significant correlations between oral-origin commensal taxa abundance in URT and LRT samples, such
345 as *Prevotella*, with prognostically favorable, lower levels of plasma inflammatory biomarkers, which may
346 indicate favorable regulation of innate immunity by such taxa.³³⁻³⁵ Our comparative analyses between
347 compartments showed much higher oral-lung than lung-gut similarity, suggesting that the oral cavity serves as
348 the primary source of microbial seeding for the lungs. However, we found that a small subset of patients had
349 enrichment for gut-origin commensal or pathogenic organisms in their LRT, which could not be fully accounted
350 for by URT colonization with similar taxa. Such patients with gut-origin bacteria enrichment in their lungs
351 (8.1%) had much worse survival than the rest of the cohort, and may represent a subset of patients in whom
352 gut-to-lung bacterial translocation may have occurred.^{36,37} Wider availability of BAL samples to investigate the
353 alveolar spaces more closely can provide more evidence into the question of gut-to-lung translocation, but our
354 non-invasive ETA samples showed that such translocation, if present, affects a small subset of patients at least
355 within the first week of IMV. Therefore, efforts focused on preventing dysbiosis and pathogen colonization in
356 the URT-to-LRT ecosystem may offer higher biological plausibility for measurable benefits in clinical trials.

357 Unsupervised clustering revealed distinct microbial communities within and across body compartments.
358 Low-diversity bacterial clusters were enriched with pathogens and depleted in anaerobes in all three
359 compartments. Membership in the low-diversity cluster was strongly associated between the oral and lung
360 compartment, suggesting shared patterns of dysbiosis. The overall stability of longitudinal cluster membership
361 indicated that specific microbial profiles may persist throughout critical illness, influencing the disease
362 trajectory. Integration of fungal sequencing data further enhanced our view of the microbial communities,
363 revealing patients who had a “double-hit” of bacterial pathogen enrichment and *C.albicans* dominance in their
364 communities. We have recently shown that *C.albicans* abundance in the LRT correlates with systemic

365 inflammation and predicts adverse outcome in patients with ARF on IMV.¹³ With the current expanded dataset,
366 we demonstrate that integration of bacterial and fungal data can identify patient subpopulations with inter-
367 kingdom dysbiosis, who may require different interventions to address both bacterial and fungal dysbiosis.

368 Survival analyses based on microbiota clusters revealed two significant and novel findings. First, in this
369 comparison of microbiota from three distinct body compartment microbiota for predicting survival in critically ill
370 patients, the lung microbiome emerged as the most powerful predictor compared to oral or gut microbiota.
371 Perhaps this finding should not be surprising when studying patients who required IMV for ARF. We had
372 previously shown that baseline lung microbiota profiles were predictive of survival.³ We now expand analyses
373 to three compartments up to three time points during IMV and show that lung microbiota carry the most
374 predictive signal for survival, both at baseline and also in follow-up samples. Thus, our comparative
375 assessment of microbiota across body compartments highlights the clinical relevance of lung microbiota
376 analysis in critical illness and the need for dedicated sampling of the LRT.³⁸ Second, the prognostic value of
377 lung microbiota clusters was independent not only from clinical predictors and validated organ dysfunction
378 metrics, such as the SOFA score, but also from the systemic host-response subphenotypes. Extensive
379 evidence has established the prognostic value and generalizability of plasma biomarker-based subphenotyping
380 of patients with ARF.^{8,39} Our adjusted Cox proportional hazards models revealed significant hazards ratios for
381 the Low-Diversity lung cluster, when analyzed using both the bacterial DMM and bacterial-fungal SNF
382 methods. Beyond the significant taxa-biomarker associations we observed, the survival analyses demonstrated
383 that lung microbiota may influence patient outcome in ways that are not captured by current host-response
384 subphenotyping approaches. An integrative, host- and lung microbiome-aware subphenotyping framework may
385 thus augment our ability to better prognosticate and target therapeutic interventions in ARF.

386 Our study has several limitations. First, we mainly focused on bacterial and fungal components of the
387 microbiome, and thus could not assess the role of the virome, especially with regards to respiratory RNA
388 viruses. The consistent pattern of results relating elements of the bacterial microbiome to host response and
389 illness severity in the COVID-19 cohorts supports the generalizability of our findings, although we could not
390 investigate contributions from individual viruses. The observational nature of our study prevents us from

391 establishing causality between the microbiome and clinical outcomes, which could be addressed by future
392 interventional studies or animal modeling with microbiome manipulation. Longitudinal sample availability was
393 limited by informative censoring, as patients with rapid decline and early death or those with rapid improvement
394 and liberation from IMV would not contribute follow-up samples in the middle and late intervals. We aimed to
395 mitigate some of these right censoring biases with mixed linear regression models, but our longitudinal
396 analysis findings should be interpreted with caution and considered as applicable to patients who remain on
397 IMV for the first 1-2 weeks of critical illness. For patient safety and practical purposes of subject participation in
398 our observational research study, we relied on non-invasive biospecimens (ETA) for LRT microbiota profiling,
399 as opposed to reference standard BAL.³⁸ Our non-invasive approach allowed us to enroll a large cohort of LRT
400 specimens, follow serial samples over time, and is congruent with clinical practice guidelines for VAP
401 diagnosis.⁴⁰ However, we may have missed important microbiota variability closer to the alveolar space,
402 including a stronger signal of gut-to-lung microbiota translocation.³⁷ Finally, we had a smaller effective sample
403 size for gut microbiota analysis, which may have limited our ability to identify prognostic variation within the gut
404 compartment.

405 In conclusion, our study provides novel insights into the predictive value of microbiota clusters derived
406 from different body compartments in critically ill patients. The lung microbiome emerged as the most powerful
407 predictor of survival, surpassing the oral and gut microbiota. These findings emphasize the clinical relevance of
408 investigating the lung microbiota and highlight its potential as a prognostic marker in critical illness. Moreover,
409 our study underscores the importance of considering organ-specific microbial communities in critical care
410 settings and expands our understanding of the microbiome's role in determining patient outcomes. Further
411 research in this area has the potential to shape clinical decision-making and facilitate the development of
412 personalized medicine strategies for critically ill patients.

413 **Online Methods**

414 UPMC-ARF cohort: Following admission to the ICU and obtaining informed consent from patients or their
415 legally authorized representatives (IRB protocol STUDY19050099), we collected baseline research
416 biospecimens within 72hrs from intubation. We collected blood for separation of plasma, oropharyngeal (oral)
417 swabs to profile upper respiratory tract (URT) microbiota, endotracheal aspirates (ETA) for LRT (lung)
418 microbiota and host biomarker measurements, and rectal swabs or stool samples for gut microbiota analyses.
419 We also captured leftover bronchoalveolar lavage fluid (BALF) from clinically indicated bronchoscopies, when
420 available. We repeated research biospecimen sampling between days 3-6 (middle interval) and days 7-12 (late
421 interval) post enrollment for subjects who remained in the ICU. No patients in the UPMC-ARF cohort were
422 known to be infected by SARS-CoV-2 at the time of enrollment.

423 UPMC-COVID cohort: Following admission to the ICU and obtaining informed consent from patients or their
424 legally authorized representatives (IRB protocol STUDY19050099), we collected baseline research
425 biospecimens (ETA and blood) within 72hrs from intubation. We repeated research biospecimen sampling
426 between days 3-6 (middle interval) and days 7-12 (late interval) post enrollment for subjects who remained in
427 the ICU, as per the UPMC-ARF protocol. All patients were known to be infected by positive SARS-CoV-2
428 qPCR prior to enrollment.

429 MGH-COVID cohort: From April 2020 to May 2021, we prospectively enrolled 97 hospitalized patients aged
430 ≥ 18 years with confirmed COVID-19 at the Massachusetts General Hospital to a longitudinal COVID-19
431 disease surveillance study.¹⁵ Patients were categorized as having severe COVID-19 if they required admission
432 to the intensive care unit with acute respiratory failure (the need for oxygen supplementation ≥ 15 liters per
433 minute (LPM), non-invasive positive pressure ventilation, or mechanical ventilation) or other organ failure (such
434 as shock requiring vasopressors). Otherwise, they were categorized as having moderate COVID-19.
435 Expecterated sputum, ETA or fresh stool was collected and refrigerated at 4°C until aliquoting/freezing at -
436 80°C (typically within 4 hours of collection) from adult patients enrolled in the prospective biospecimen
437 collection study. Participants were able to provide samples as frequently as once daily for up to four days, as
438 well as declining donation on any given day (while remaining in the study).

439 Healthy Controls: To contextualize the findings on microbiota from critically-ill patients with what is expected for
440 the healthy respiratory and gastrointestinal tract, we also included data from 24 healthy volunteers who had
441 contributed URT and LRT microbiome data in a previously published cohort (Lung HIV Microbiome Project -
442 STUDY19060243),⁴¹ as well as stool from 15 healthy donors for fecal microbiota transplantation.¹¹ We
443 designated these healthy volunteers as Healthy Controls.

444 Clinical data recording: A consensus committee reviewed clinical and radiographic data and performed
445 retrospective classifications of the etiology and severity of acute respiratory failure without knowledge of
446 microbiome sequencing or biomarker data. We retrospectively classified subjects as having ARDS per
447 established criteria (Berlin definition), being at risk for ARDS because of the presence of direct (pneumonia or
448 aspiration) or indirect (e.g., extrapulmonary sepsis or acute pancreatitis) lung-injury risk factors although
449 lacking ARDS diagnostic criteria, having acute respiratory failure without risk factors for ARDS, or having
450 acute-on-chronic respiratory failure. We followed patients prospectively for cumulative mortality and ventilator-
451 free days (VFDs) at 30 days, as well as survival up to 60 days from intubation.

452 We systematically reviewed administered antibiotic therapies since hospital admission and recorded the
453 antibiotic exposure for each subject according to the following three metrics:

- 454 1. Anaerobic coverage (yes/no): whether antibiotics with anaerobic coverage were given on the day of
455 sampling.
- 456 2. The Antibiotic Exposure score by Zhao et al ¹⁶: a numerical scale with antibiotic weighting based on
457 dosing duration, timing of administration relative to sample collection and antibiotic type and route of
458 administration. We utilized the convex increasing weighting scheme and modeled the antibiotic
459 exposure from hospital admission until day of sampling.
- 460 3. The Narrow Antibiotic Treatment (NAT) score developed for community-acquired pneumonia treatment
461 studies ^{17,25}. We calculated the daily NAT score from -5 days from sampling to post 10 days after
462 sampling on day 1.

463
464 Research Sample Collection

465 Within the first 48 hours of intubation (baseline time-point), we collected a posterior oropharyngeal
466 (oral) swab via gentle swabbing the posterior oropharynx next to the endotracheal tube with a cotton tip swab
467 for 5 secs, and an endotracheal aspirate (ETA) via suctioning secretions from the endotracheal tube with the
468 in-line suction catheter and without breaking seal in the ventilatory circuit.^{1,4} Rectal swabs were collected
469 according to a standard operating procedure (i.e., placing the patient in a lateral position, inserting the cotton
470 tip of the swab into the rectal canal, and rotating the swab gently for 5 s), unless clinical reasons precluded
471 movement of the patient (e.g., severe hemodynamic or respiratory instability). Stool samples were collected
472 when available, either by taking a small sample from an expelled bowel movement (before cleaning of the
473 patient and disposal of the stool) or from a fecal management system (rectal tube) placed for management of
474 diarrhea and liquid stool collection. We also collected simultaneous blood samples for centrifugation and
475 separation of plasma, which was stored in -80C until conduct of experiments. For patients who remained
476 intubated in the ICU, we collected follow-up samples at a middle time-point (days 3-6) and a late follow-up
477 interval (days 7-11 post-intubation).

478 For Healthy Controls, an oral wash and BAL sample were collected with a standardized protocol.⁴¹
479 Subjects were asked to fast and refrain from smoking for at least 12hrs before sample collection. Oral washes
480 were performed by having participants gargle with 10 ml sterile 0.9% saline immediately before bronchoscopy.
481 BAL was performed according to standardized procedures developed to minimize oral contamination.
482 Participants gargled with an antiseptic mouthwash (Listerine) immediately before topical anesthesia. The
483 bronchoscope was then inserted through the mouth and advanced to a wedge position quickly and without use
484 of suction. BAL was performed in the right middle lobe or lingula up to a maximum of 300 ml 0.9% saline.
485 Healthy donors of stool for fecal microbiota transplant collected a stool sample in a specialized container and
486 brought the stool sample on the day of collection to the processing lab.

488 *Laboratory Analyses*

489 Microbiome assays in UPMC cohorts: From oral swabs, ETAs, left over BALF, rectal swabs and stool samples,
490 we extracted genomic DNA and performed quantitative PCR (qPCR) of the V3-V4 region of the 16S rRNA
491 gene to obtain the number of gene copies per sample, as a surrogate for bacterial load. From a separate

492 aliquot of extracted DNA from oral swabs, ETA, rectal swabs and stool samples, we performed amplicon
493 sequencing for bacterial DNA (16S-Seq of the V4 hypervariable region) and fungal DNA (ITS) on the Illumina
494 MiSeq platform.^{3,42} We used extensive experimental negative controls in all processing steps to rule out
495 contamination, as well as mock microbial community positive controls (Zymo) to ensure target amplification
496 success. We processed derived 16S sequences with a custom Mothur-based pipeline and performed analyses
497 at genus level. From a random subset of 130 available ETA samples, we performed metagenomic Nanopore
498 sequencing (following human DNA depletion) with a rapid PCR barcoding kit (SQK-RPB004) on the MinION
499 device (Oxford Nanopore Technologies-ONT, Oxford, UK) for five hours.^{43,44} We analyzed microbial
500 metagenomic sequences with the EPI2ME platform (ONT) and the “What’s In My Pot” [WIMP] workflow to
501 quantify abundance of microbial species.⁴⁵ We filtered FASTQ files with a mean quality (q-score) below a
502 minimum threshold of 7.

503 Host-response assays: We measured 10 plasma biomarkers of tissue injury and inflammation with custom
504 Luminex multi-analyte panels from plasma samples and ETA supernatants, when available. Specifically, we
505 used a 10-plex Luminex panel (R&D Systems, Minneapolis, MI, United States) to measure interleukin(IL)-6, IL-
506 8, IL-10, soluble tumor necrosis factor receptor 1 (sTNFR1), suppressor of tumorigenicity-2 (ST2), fractalkine,
507 soluble receptor of advanced glycation end-products (sRAGE), angiopoietin-2, procalcitonin and pentraxin-3.⁷

508 Microbiome assays in MGH-COVID cohort: Samples were extracted and sequenced at Baylor College of
509 Medicine according to their standard established platforms. DNA was prepared for sequencing using the
510 Illumina Nextera XT DNA library preparation kit. All libraries were sequenced with a target of 3GB output at
511 2x150bp read length using the Illumina NovaSeq platform, as previously described.¹⁵

512 Quantification and statistical analysis.

514 We performed non-parametric comparisons for continuous (described as median and interquartile
515 range – IQR) and categorical variables between clinical groups (Wilcoxon and Fisher’s exact tests,
516 respectively). For microbial community profiling, we included samples that produced >300 high quality
517 microbial reads for both 16S-Seq and Nanopore sequencing. We performed alpha diversity (Shannon index)
518 calculations for each available sample, and then conducted between group comparisons of alpha diversity with

519 non-parametric tests to draw inferences on systematic differences of alpha diversity between groups as a
520 measure of relative community fitness.¹ We conducted beta diversity analyses (Manhattan distances, analyzed
521 via permutation analysis of variance and visualized via principal coordinates analyses) with the R *vegan* and
522 *mia* packages.⁴⁶ We examined for differentially abundant taxa between groups following centered log-ratio
523 (CLR) transformations with the *limma* package to fit weighted linear regression models, perform tests based on
524 an empirical Bayes moderated *t*-statistic and obtain False Discovery Ratio corrected p-values.

525 We then examined the discovered bacterial taxa at genus level and classified them by two different
526 classification schemes with clinical relevance¹²:

527 A. By oxygen requirements for bacterial metabolism:

- 528 1. Obligate aerobes (referred to throughout as aerobes): bacteria that require oxygen to grow
529 and survive, as they use oxygen as final electron acceptor in their respiratory chain.
- 530 2. Obligative anaerobes (referred to throughout as anaerobes): bacteria that are unable to
531 grow in the presence of oxygen, as they are unable to use oxygen as a final electron
532 acceptor and are killed in the presence of oxygen.
- 533 3. Facultative anaerobes: bacteria that can grow in the presence or absence of oxygen. They
534 can use both aerobic and anaerobic respiration, depending on the availability of oxygen in
535 their environment, switching from aerobic to anaerobic metabolism.
- 536 4. Microaerophiles: bacteria that require a low level of oxygen to grow and survive, as they can
537 grow at oxygen concentrations lower than those required by obligate aerobes but higher
538 than those tolerated by obligate anaerobes.
- 539 5. Variable: genera that included both aerobes and anaerobes and could not be classified
540 further with confidence.
- 541 6. Unclassifiable: taxa that were not classified at the genus or family level with confidence to
542 allow assessment of their metabolic needs.

543 B. By pathogenicity for LRT infections:

- 544 1. Common respiratory pathogens: bacteria considered to be typical pathogens when isolated
545 in LRT microbiologic cultures.

2. Oral-origin commensal bacteria: bacterial taxa that have been characterized as typical members of the lung microbiome in health and originate from the oral cavity.
3. Other: taxa with unclear clinical significance that do not fall into categories B1 or B2 above.

To agnostically examine our samples for distinct clusters of microbial composition (“metacomunities”), we applied unsupervised Dirichlet multinomial models (DMMs) with Laplace approximations¹⁸ to define the optimal number of clusters in our dataset, and then examined for associations with clinical parameters and outcomes. To synthesize bacterial and fungal data within each compartment, as well as bacterial profiles across different compartments, we used the weighted Similarity Network Fusion function.¹⁹ We classified subjects into a hyper- vs. hypo-inflammatory subphenotype based on predictions from a parsimonious logistic regression model utilizing plasma levels of sTNFR1, Ang-2 and procalcitonin (research biomarkers measured with Luminex panel), as well as serum bicarbonate levels measured during clinical care.

We followed patients prospectively and constructed Kaplan-Meier curves and Cox-proportional hazard models for 60-day survival, adjusted for the predictors of age and sex, as well as plausible confounders of microbiome associations diagnosis based on our findings (history of COPD, history of Immunosuppression), severity of illness as per the SOFA score, and host-response subphenotypes. To examine for the impact of mechanical ventilation, steroids and antibiotics pressure on longitudinal microbiota profiles, we constructed mixed regression models with random patient intercepts and adjusted for the number of days post-intubation that each sample was taken (as a proxy for the exposure to the hyperoxic environment of the ventilator) and the antibiotic exposure and steroids metrics by the day of sampling. We performed all statistical analyses in R v.4.2.0.⁴⁷

Following derivation of the DMM clusters in each compartment of the UPMC-ARF cohort and demonstration of significant associations with patient outcomes, we proceeded to develop multinomial logistic regression models for prediction of classification of bacterial 16S profiles from new samples into predicted cluster assignments. We considered these new classification models as a Dysbiosis Index for each compartment. To develop these models in each compartment (oral, lung and gut), we used probabilistic graphical modeling (PGM)⁴⁸ by considering the 50 most abundant taxa in each compartment along with the Shannon Index. We divided the samples of each compartment into two random subsets: 80% of data points for

training and 20% for testing. The training set was used to generate a PGM using the FCI-MAX algorithm with Alpha of 0.1 to examine which variables (50 taxa abundance and Shannon Index) were associated with the cluster assignments in each compartment. The variables that appeared in the Markov blanket of the DMM cluster assignment variable were used to create a multinomial logistic regression (MLR) model to predict the cluster assignment of future samples. The MLR model equations were written as follows for the different cluster assignments (Low, Intermediate and High Diversity):

Model equations

$$\ln \left(\frac{P(\text{Intermediate})}{P(\text{HighDiversity})} \right) = b_{10} + b_{11} \cdot f_1 + \dots + b_{1n} \cdot f_n \quad \text{Equation 1}$$

$$\ln \left(\frac{P(\text{LowDiversity})}{P(\text{HighDiversity})} \right) = b_{20} + b_{21} \cdot f_1 + \dots + b_{2n} \cdot f_n \quad \text{Equation 2}$$

f: feature

b1 & b2 are model coefficients

By rewriting the equations, we get the following:

$$\frac{P(\text{Intermediate})}{P(\text{HighDiversity})} = e^{(b_{10} + b_{11} \cdot f_1 + \dots + b_{1n} \cdot f_n)} \quad \text{Equation 3}$$

$$\frac{P(\text{LowDiversity})}{P(\text{HighDiversity})} = e^{(b_{20} + b_{21} \cdot f_1 + \dots + b_{2n} \cdot f_n)} \quad \text{Equation 4}$$

We rewrote the names of the model parameters as :

$$P(\text{HighDiversity}) = P(H)$$

$$P(\text{Intermediate}) = P(I)$$

$$P(\text{LowDiversity}) = P(L)$$

$$e^{(b_{10} + b_{11} \cdot f_1 + \dots + b_{1n} \cdot f_n)} = X$$

$$e^{(b_{20} + b_{21} \cdot f_1 + \dots + b_{2n} \cdot f_n)} = Y$$

We know that $P(H) + P(I) + P(L) = 1$ Equation 5

Then $P(H) = 1 - P(I) - P(L)$ Equation 6

From Equation 3 and 4

$$P(I) = X P(H)$$

$$P(H) = \frac{P(L)}{Y}$$

Substituting in Equation 6

$$\frac{P(L)}{Y} = 1 - X \frac{P(L)}{Y} - P(L)$$

$$\frac{P(L)}{Y} + X \frac{P(L)}{Y} + P(L) = 1$$

612
613
614
615
616
617
618
619
620
621
622

$$P(L) \left[\frac{1}{Y} + \frac{X}{Y} + 1 \right] = 1$$

$$P(L) \left[\frac{1 + X + Y}{Y} \right] = 1$$

$$P(L) = \left[\frac{Y}{1 + X + Y} \right]$$

$$P(H) = \left[\frac{1}{1 + X + Y} \right]$$

$$P(I) = \left[\frac{X}{1 + X + Y} \right]$$

The predicted cluster is the one with the highest probability. For example, if $\max(P(H), P(I), P(L)) = P(I)$, then the predicted cluster is $P(I)$

The Intercepts and co-efficients for the MLR models for each compartment are provided below.

Oral		
<i>f</i>	<i>b</i> ₁	<i>b</i> ₂
Intercept	8.124887	13.323657
ShannonIndex	-1.57054	-2.79173
Actinomyces	0.4883585	0.1975639
Capnocytophaga	0.1550266	-0.2497556
Fusobacterium	0.04705918	-0.49428753
Granulicatella	0.03521261	-0.22396119
Leptotrichia	-0.5982385	-0.6815710
Parvimonas	-0.8593016	-0.6830944
Porphyromonas	-0.7968399	-0.4426564
Prevotellaceae_uncl	-0.3983984	-1.9055700
Stomatobaculum	-0.5966283	-1.3445377

623

Lung		
<i>f</i>	<i>b</i> ₁	<i>b</i> ₂
Intercept	6.091456	13.161966
ShannonIndex	-2.235179	-3.955922
Streptococcus	0.08810083	-0.30461314
Veillonella	0.27052525	0.04224102
Peptostreptococcus	-0.02538055	0.50470722
Porphyromonas	-0.520896	-1.387346
Selenomonas	-0.5639481	-1.2279826
Alloprevotella	-0.4193465	-1.0781599
Leptotrichia	-0.09918638	-1.16197619
Neisseriaceae_uncl	-0.430702	-1.654160

624

Gut		
<i>f</i>	<i>b</i> ₁	<i>b</i> ₂
Intercept	-0.7901505	4.5913451
ShannonIndex	2.104042	-1.017060
Atopobium	1.0404839	0.1382178
Streptococcus	-0.1680732	0.2080845

Enterococcus	-0.04209851	0.38397607
Faecalibacterium	-0.8249428	-0.9945793
Fenollaria	0.4178598	-0.5862931
Alistipes	-1.3291409	-0.6846156
Lachnospiraceae uncl	-1.1289312	-0.7073528

625

626

We tested the MLR model using three datasets: The 20% testing set for estimating model accuracy, and the

627

ALIR-COVID samples and the MGH-COVID samples for examining associations between the Dysbiosis Index

628

with clinical variables and endpoints.

629

Applications of the MLR models (Dysbiosis Index) in the three compartments showed the following accuracy

630

statistics (95% confidence intervals) for prediction of the DMM clusters:

631

Oral Dysbiosis Index: 0.76 (0.65-0.85)

632

Lung Dysbiosis Index: 0.86 (0.76-0.93)

633

Gut Dysbiosis Index: 0.75 (0.60-0.86)

634

635 **Acknowledgements:**

636 The authors wish to thank the patients and patient families that have enrolled in the University of Pittsburgh
637 Acute Lung Injury Registry. We also thank the physicians, nurses, respiratory therapists and other staff at the
638 University of Pittsburgh Medical Center Presbyterian, Shadyside and East Hospitals intensive care units for
639 assistance with coordination of patient enrollment and collection of patient samples. We would like to thank the
640 laboratory personnel at the Center for Medicine and the Microbiome at the University of Pittsburgh for
641 assistance with processing clinical samples. We acknowledge the contributions of Nameer Al-Yousif, MD,
642 Michael Lu, MD, Grace Lisius MD, and Caitlin Shaefer, MPH who participated in clinical data extractions for
643 specific components of the databases of the UPMC-ARF and UPMC-COVID cohorts. We also thank the
644 Massachusetts General Hospital Translational and Clinical Research Center (TCRC) for their support of the
645 project and the assembly of the MGH-COVID cohort.

646 **Ethics approval and consent to participate:** The University of Pittsburgh Institutional Review Board (IRB)
647 approved the protocol for the UPMC-ARF and UPMC-COVID cohorts (STUDY19050099). We obtained written
648 or electronic informed consent by all participants or their surrogates in accordance with the Declaration of
649 Helsinki. For the MGH-COVID cohort, the Study protocol #2020P000804 was approved by the Mass General
650 Brigham IRB. All participants or their healthcare proxy provided written informed consent to participate.
651

652

653 **Consent for publication:** We obtained necessary patient/participant consent and the appropriate institutional
654 forms have been archived. Any patient/participant/sample identifiers included were not known to anyone
655 outside the research group so cannot be used to identify individuals.

656

657 **Data and code availability:**

658 Sequencing data collected for the study have been deposited to the Sequencing Resource Archive, through
659 the following Accession numbers:

660 -PRJNA595346 for 16S data of UPMC-ARF and UPMC-COVID cohorts (477 records released and remainder
661 to be released upon publication with Temporary Submission ID SUB13319619),

662 -PRJNA726955 for ITS data of UPMC-ARF cohort,

663 -PRJNA554461 for Nanopore data of UPMC-ARF cohort,
664 -PRJNA940725 for 16S data of the Healthy Controls,
665 -PRJNA976404 for Metagenomic data of the MGH-COVID cohort.
666 Primary code and de-identified data for replication of analyses will be available on the github repository
667 (<https://github.com/MicrobiomeALIR/MultiCompartmentMicrobiome>) upon acceptable of the manuscript for
668 publication. Any additional information required to reanalyze the data reported in this paper is available from
669 the lead contact upon request.

670

671

672

Table 1: Baseline characteristics of enrolled mechanically ventilated patients in the UPMC-ARF cohort, stratified by 60-day mortality. We compared continuous variables with non-parametric Wilcoxon tests and categorical variables with Fisher's exact tests between the three groups. Statistically significant differences ($p < 0.05$) are highlighted in bold.

	All	Survivors	Non-Survivors	p
N	479	350	129	
Age, years (median [IQR])	59.6 [46.7, 68.7]	57.1 [44.1, 67.1]	65.3 [55.8, 72.2]	<0.01
Men, n (%)	256 (54.4)	180 (52.6)	76 (58.9)	0.26
Whites, n (%)	425 (90.2)	307 (89.8)	118 (91.5)	0.67
BMI (median [IQR])	29.4 [25.5, 36.0]	29.6 [25.5, 35.7]	28.6 [25.3, 36.6]	0.98
COPD, n (%)	104 (22.1)	75 (21.9)	29 (22.5)	1.00
Diabetes, n (%)	168 (35.7)	122 (35.7)	46 (35.7)	1.00
Alcohol use, n (%)	84 (17.9)	60 (17.5)	24 (18.9)	0.84
Immunosuppression, n (%)	105 (22.3)	71 (20.8)	34 (26.4)	0.24
ARDS, n (%)	117 (25.2)	81 (24.0)	36 (28.1)	0.23
WBC (median [IQR])	12.0 [8.7, 16.8]	11.4 [8.1, 15.8]	14.4 [10.1, 18.7]	<0.01
Creatinine (median [IQR])	1.2 [0.8, 2.3]	1.1 [0.8, 2.0]	1.6 [0.9, 2.5]	0.01
Plateau Pressure (median [IQR])	20.0 [16.0, 25.0]	19.0 [16.0, 24.0]	22.0 [18.0, 27.0]	<0.01
PaO ₂ :FiO ₂ ratio (median [IQR])	164.0 [117.0, 206.0]	168.0 [121.5, 211.0]	157.0 [108.0, 205.0]	0.04
SOFA scores (median [IQR])	6.0 [4.0, 9.0]	6.0 [4.0, 8.0]	8.0 [5.0, 10.0]	<0.01
LIPS score (median [IQR])	5.5 [4.0, 6.5]	5.0 [4.0, 6.5]	6.0 [5.0, 7.5]	<0.01
Hypoinflammatory subphenotype, n (%)	344 (75.6)	254 (77.4)	90 (70.9)	0.18
VFD (median [IQR])	22.0 [13.0, 25.0]	23.0 [20.0, 25.2]	0.0 [0.0, 19.0]	<0.01

Abbreviations: IQR: Interquartile Range; BMI: body mass index; COPD: chronic obstructive pulmonary disease, LIPS: lung injury prediction score; WBC: white blood cell count; PaO₂: partial pressure of arterial oxygen; FiO₂: Fractional inhaled concentration of oxygen; SOFA: sequential organ failure assessment; VFD: ventilator free days; ARDS: acute respiratory distress syndrome.

685 **Figures:**

686 **Figure 1. Ecological features of dysbiosis in three body compartments in critically ill patients. A.**

687 Samples from critically ill patients had significantly lower alpha diversity (Shannon index) compared to

688 corresponding healthy control samples in each compartment ($p < 0.001$), with further decline of Shannon index

689 over time in longitudinal samples ($p < 0.001$). B. Baseline samples from critically ill patients had markedly

690 significant differences in beta diversity from healthy controls (permutational analysis of variance [permanova]

691 p-values < 0.001). C-E. Taxonomic composition comparisons with the *limma* package showed high effect sizes

692 and significance thresholds (threshold of log₂-fold-change [log₂FC] of centered-log-transformed [CLR]

693 abundances > 1.5 ; Benjamini-Hochberg adjusted p-value < 0.05) showed depletion for multiple commensal taxa

694 in critically ill patients samples, with significant enrichment for *Staphylococcus* in oral and lung samples, and

695 *Anaerococcus* and *Enterococcus* in gut samples (significant taxa shown in red in the volcano plots). F. Lung

696 samples had lower bacterial burden compared to oral and gut samples by 16S qPCR (all $p < 0.001$). G. Oral

697 and lung samples had higher compositional similarity (Bray-Curtis indices) compared to lung and gut samples

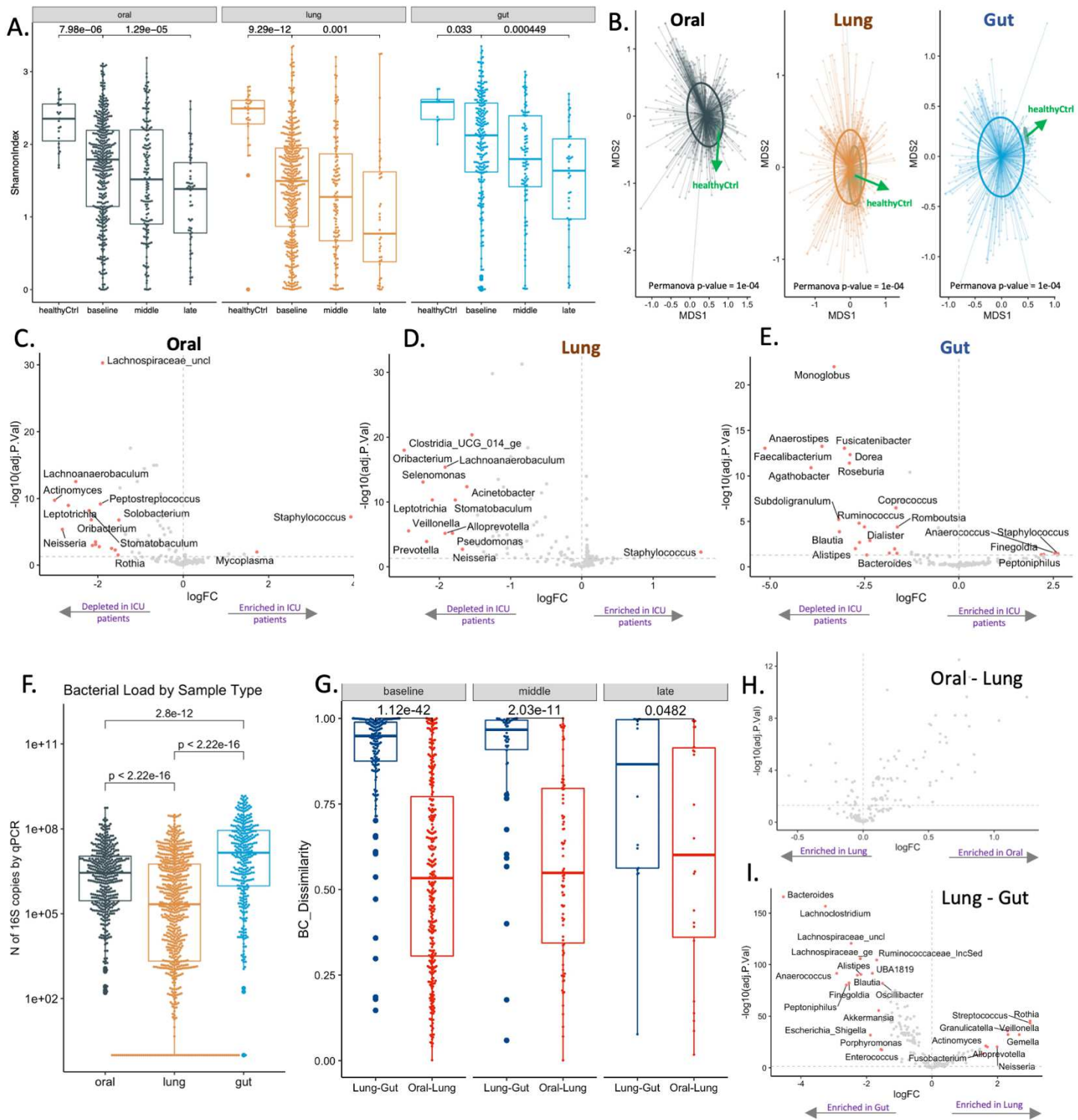
698 in the baseline and middle interval ($p < 0.001$). H-I: Taxonomic comparisons between compartments revealed

699 that no specific taxa were systematically different between oral and lung microbiota (H), whereas in gut-lung

700 comparisons, lung communities were enriched for typical respiratory commensals (e.g. *Rothia*, *Veillonella*,

701 *Streptococcus*) and gut communities for gut commensals (e.g. *Bacteroides*, *Lachnospiraceae*,

702 *Lachnospiraceae*) (I).



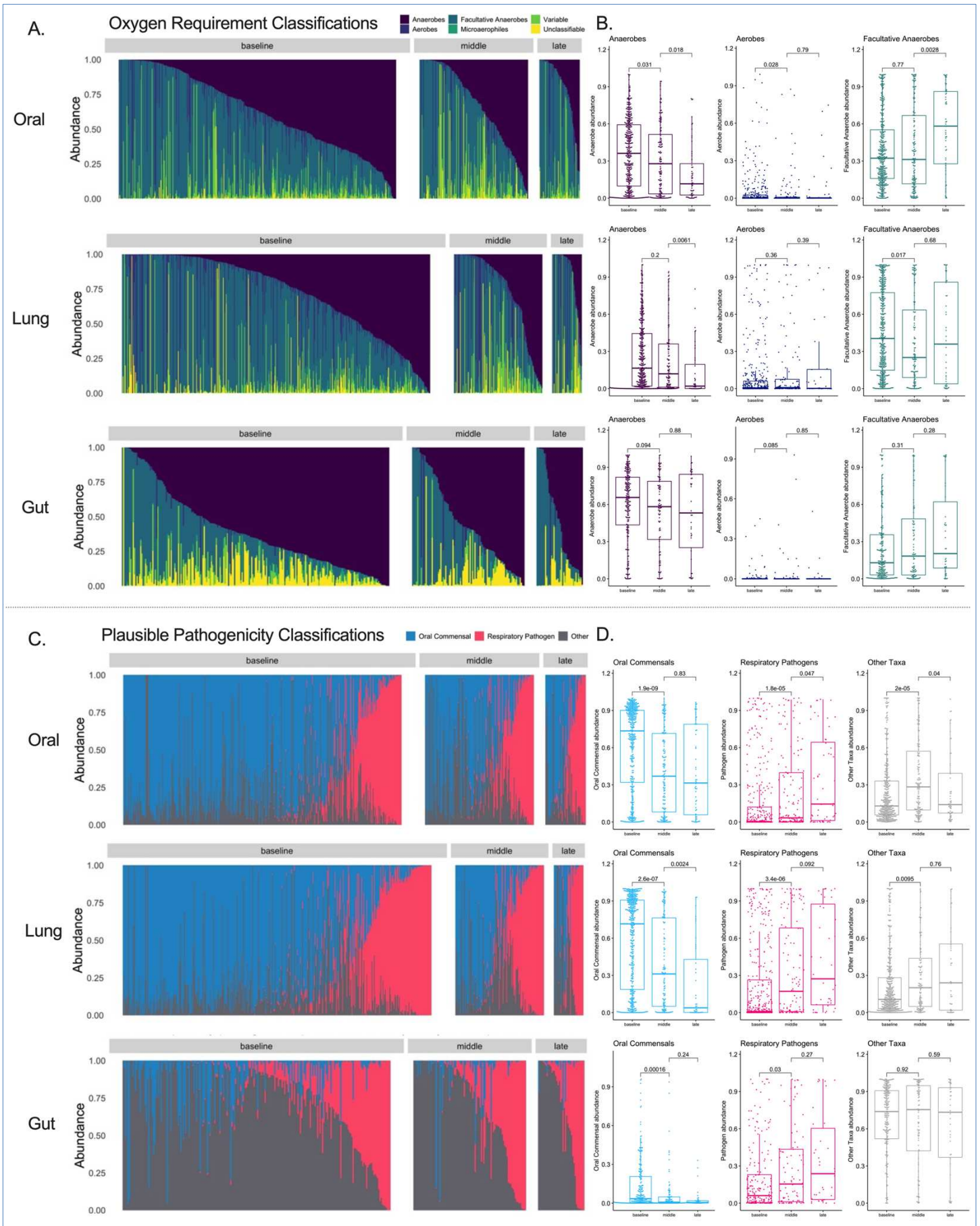
703

704

705

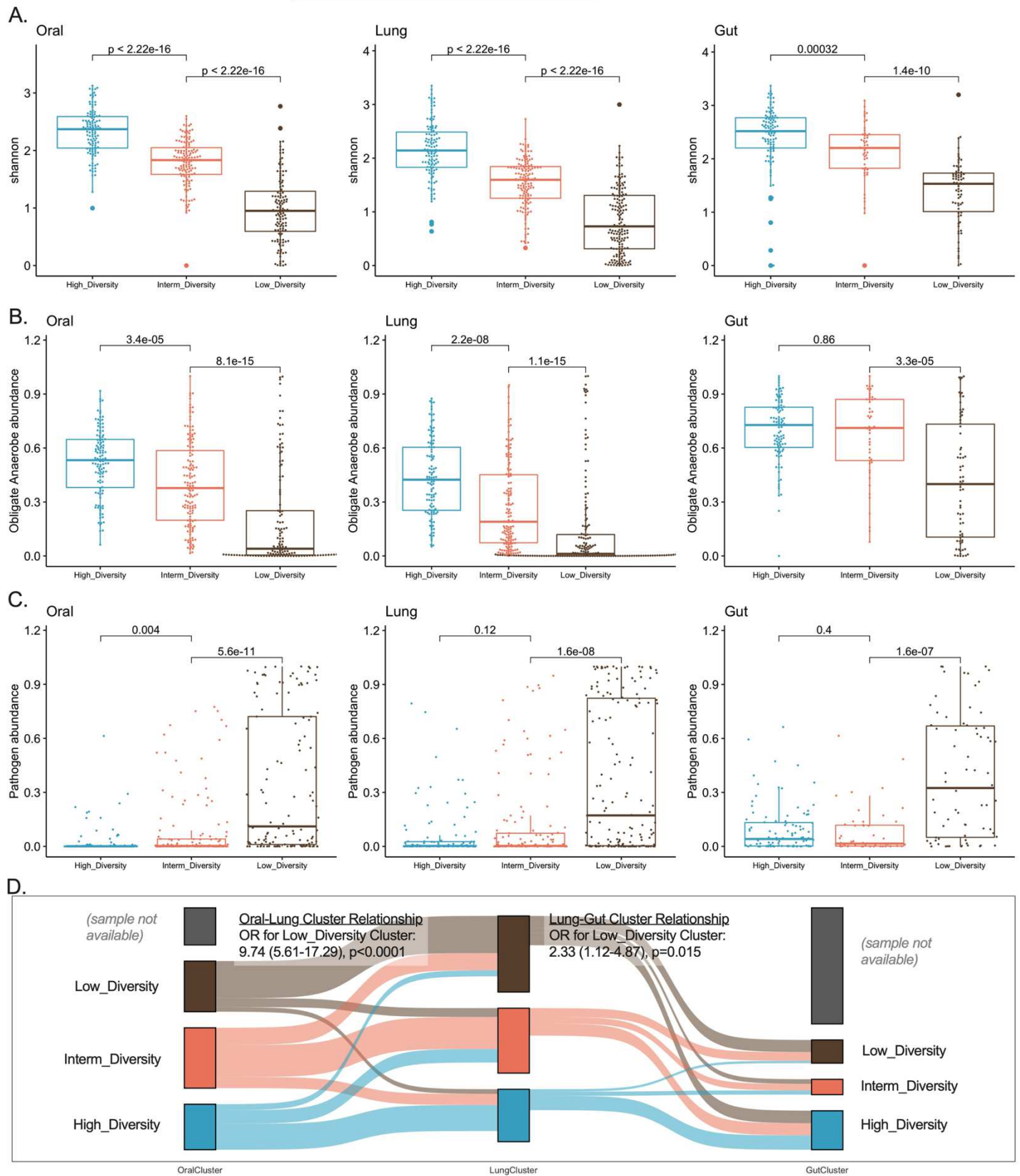
706

707 **Figure 2: Longitudinal analysis of bacterial composition showed a progressive loss of obligate**
708 **anaerobes in oral and lung communities as well as enrichment for recognized respiratory pathogens in**
709 **all three compartments.** Top Panels (A-B): Relative abundance barplots for oral, lung and gut samples with
710 classification of bacterial genera by oxygen requirement into obligate anaerobes (anaerobes), aerobes,
711 facultative anaerobes, microaerophiles, genera of variable oxygen requirement and unclassifiable.
712 Comparisons of relative abundance for the three main categories of bacteria (obligate anaerobes, aerobes and
713 facultative anaerobes) by follow-up interval (baseline, middle and late). Data in boxplots (B) are represented as
714 individual values with median values and interquartile range depicted by the boxplots with comparisons
715 between intervals by non-parametric tests. Bottom Panels (C-D): Relative abundance barplots for oral, lung
716 and gut (F) samples with classification of bacterial genera by plausible pathogenicity into oral commensals,
717 recognized respiratory pathogens and “other” category. Comparisons of relative abundance for these
718 categories of bacteria by follow-up interval (baseline, middle and late) in boxplots (D).



720 **Figure 3: Unsupervised clustering approaches revealed differences in bacterial alpha diversity and**
721 **composition in three body compartments of critically ill patients.** Panels A-D demonstrate bacterial
722 Dirichlet Multinomial Mixture (DMM) modeling results for each compartment separately. DMM clusters had
723 significant differences in alpha diversity (A) and composition (obligate anaerobe abundance in shown in panel
724 B and pathogen abundance shown in panel C), with cluster 3 in each compartment showing very low Shannon
725 Index and enrichment for pathogens (Low-Diversity cluster). Oral and lung cluster assignments were strongly
726 associated (Odds ratio for assignment to the Low-Diversity cluster: 9.74 (5.61-17.29), $p < 0.0001$), whereas lung
727 and gut cluster assignments were less strongly but significantly associated (panel D).
728

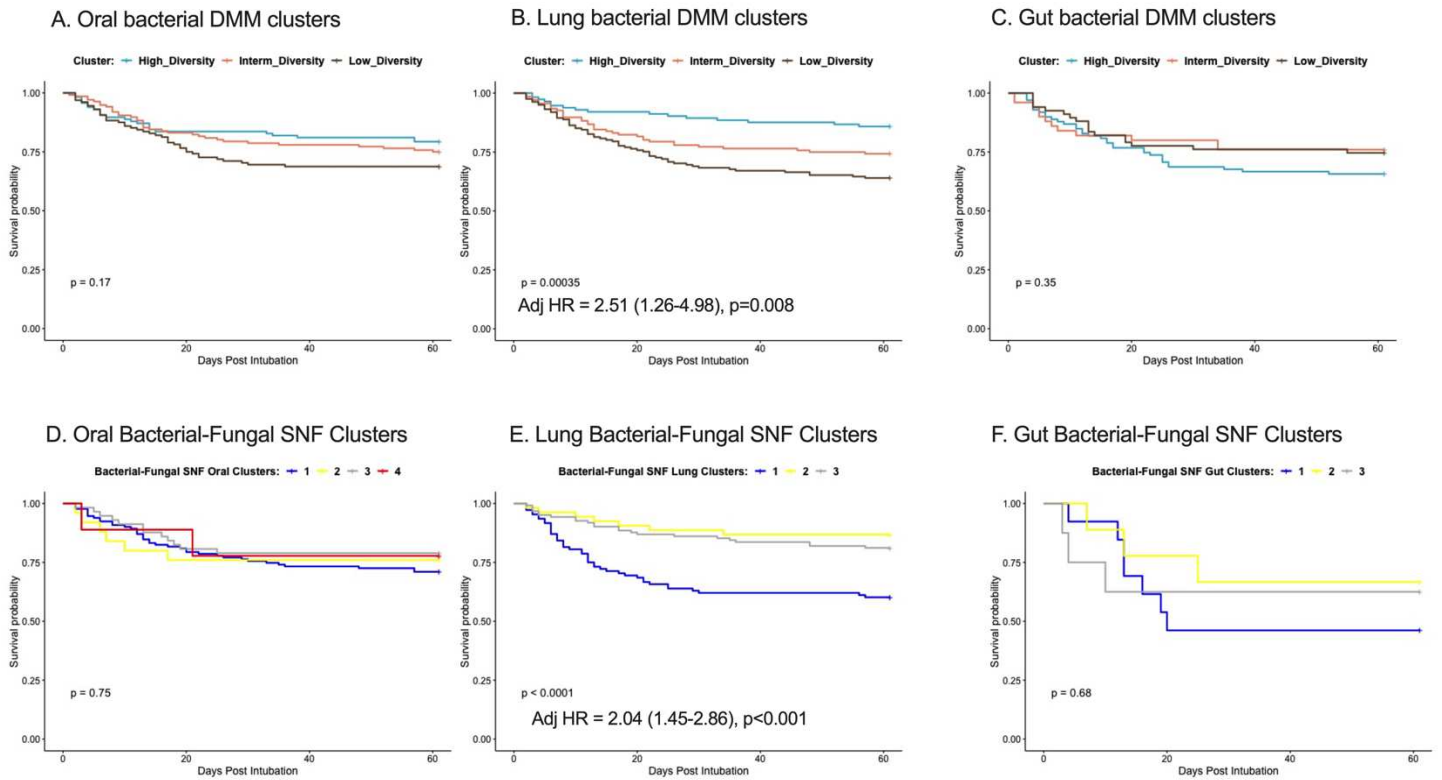
Bacterial DMM Clusters



729

730

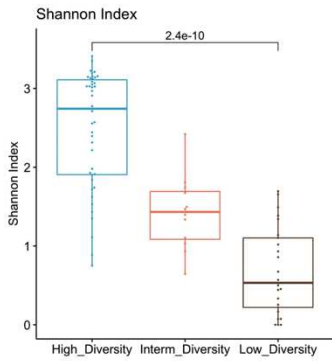
731 **Figure 4: Lung bacterial and bacterial-fungal clusters strongly predicted 60-day survival independent**
732 **of clinical predictors, organ dysfunction severity and host-response subphenotypes.** A-C: Kaplan-Meier
733 curves for 60-day survival from intubation stratified by oral (A), lung (B) and gut (C) bacterial DMM clusters.
734 The Low-Diversity lung DMM cluster was independently predictive of worse survival (adjusted Hazard Ratio =
735 2.51 (1.26-4.98), $p=0.008$), following adjustment for age, sex, history of COPD, immunosuppression, severity
736 of illness by sequential organ failure assessment (SOFA) scores and host-response subphenotypes. The Lung
737 bacterial-fungal SNF cluster with high pathogen and *C. albicans* abundance (cluster 1) was independently
738 predictive of worse survival (D), whereas the oral and gut bacterial-fungal SNF clusters (D, F) did not impact
739 survival.



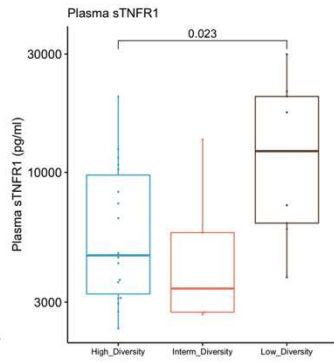
744 **Figure 5: Lung and Gut Microbiota Associations with COVID-19 Severity in Two Independent Cohorts.**

745 A. Application of the dysbiosis index in lung (ETA) microbiota profiles in the UPMC-COVID cohort classified
746 subjects in three clusters, with significant differences in Shannon index and bacterial load by 16S qPCR. B.
747 The low diversity cluster in lung samples from UPMC-COVID subjects was significantly associated with higher
748 plasma levels of sTNFR1 and Ang-2. C-D. Application of the dysbiosis index models in lung (sputum or ETA)
749 and gut (stool) samples in the MGH-COVID cohort classified subjects in three clusters, with significant
750 differences in Shannon index and anaerobe abundance between clusters. E-F: Cluster assignments in the
751 MGH cohort were strongly associated with clinical severity for lung samples only. Membership in the Low-
752 Diversity cluster in the lungs was associated with an odds ratio of 8.77 (1.75-61.74) for severe disease (black
753 belt connecting the Low-Diversity cluster and Severe Disease perimetric zones in the chord diagram). Gut
754 clusters were not significantly associated with clinical severity of COVID-19 pneumonia.

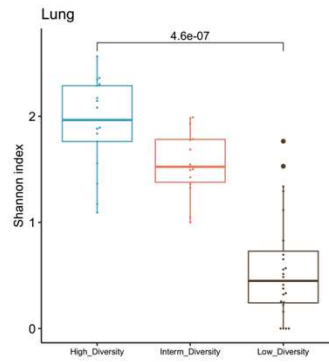
A. UPMC-COVID Lung Clusters



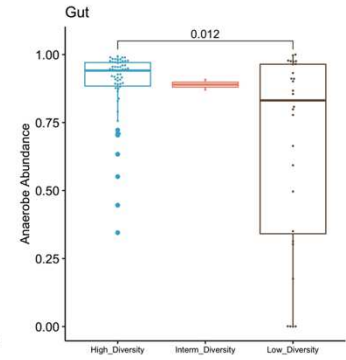
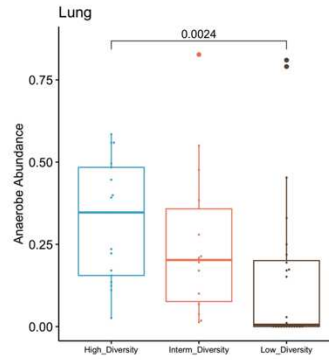
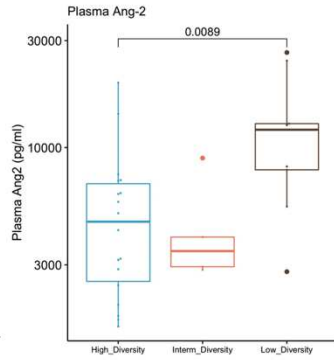
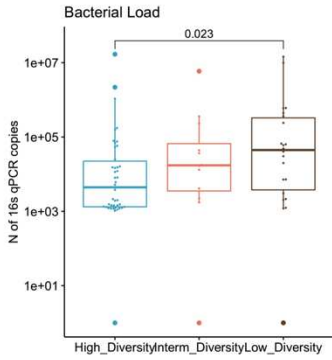
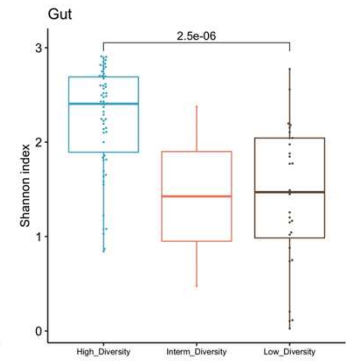
B. Lung Clusters and Plasma Host-Response Biomarkers



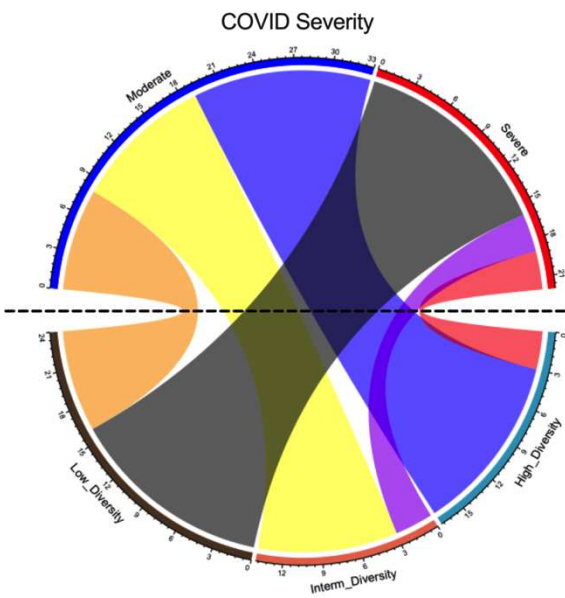
C. MGH-COVID Lung Clusters



D. MGH-COVID Gut Clusters



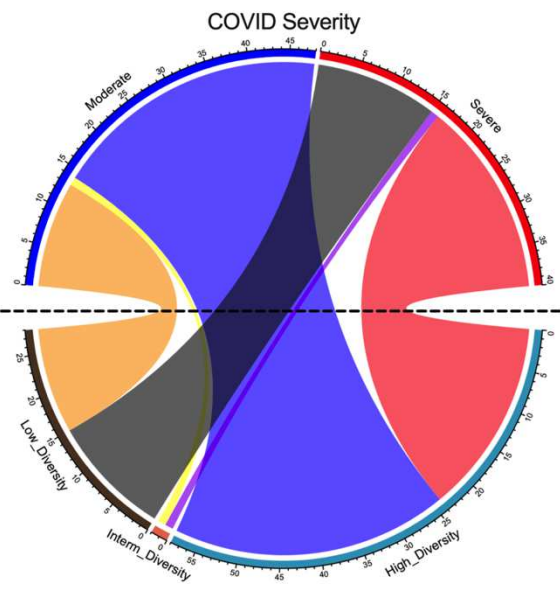
E. MGH-COVID Lung Clusters and Severity



Lung Clusters

OR = 8.77 (1.75-61.74), p=0.003, Low vs. High

F. MGH-COVID Gut Clusters and Severity



Gut Clusters

OR = 1.62 (0.59-4.47), p=0.35, Low vs. High

755
756
757
758
759

760
761 REFERENCES
762
763
764

- 765 1. Kitsios, G. D. *et al.* Dysbiosis in the intensive care unit: Microbiome science coming to the bedside. *J.*
766 *Crit. Care* **38**, 84–91 (2017).
- 767 2. Dickson, R. P. The microbiome and critical illness. *Lancet Respir. Med.* **4**, 59–72 (2016).
- 768 3. Kitsios, G. D. *et al.* Respiratory Tract Dysbiosis Is Associated with Worse Outcomes in Mechanically
769 Ventilated Patients. *Am. J. Respir. Crit. Care Med.* **202**, 1666–1677 (2020).
- 770 4. Dickson, R. P. *et al.* Lung microbiota predict clinical outcomes in critically ill patients. *Am. J. Respir.*
771 *Crit. Care Med.* **201**, 555–563 (2020).
- 772 5. Sulaiman, I. *et al.* Microbial signatures in the lower airways of mechanically ventilated COVID-19
773 patients associated with poor clinical outcome. *Nat. Microbiol.* **6**, 1245–1258 (2021).
- 774 6. Sarma, A., Calfee, C. S. & Ware, L. B. Biomarkers and precision medicine: state of the art. *Crit. Care*
775 *Clin.* **36**, 155–165 (2020).
- 776 7. Kitsios, G. D. *et al.* Host-Response Subphenotypes Offer Prognostic Enrichment in Patients With or at
777 Risk for Acute Respiratory Distress Syndrome. *Crit. Care Med.* **47**, 1724–1734 (2019).
- 778 8. Alipanah, N. & Calfee, C. S. Phenotyping in acute respiratory distress syndrome: state of the art and
779 clinical implications. *Curr. Opin. Crit. Care* **28**, 1–8 (2022).
- 780 9. Heijnen, N. F. L. *et al.* Biological Subphenotypes of Acute Respiratory Distress Syndrome Show
781 Prognostic Enrichment in Mechanically Ventilated Patients without Acute Respiratory Distress
782 Syndrome. *Am. J. Respir. Crit. Care Med.* **203**, 1503–1511 (2021).
- 783 10. Kitsios, G. D. *et al.* Distinct profiles of host responses between plasma and lower respiratory tract
784 during acute respiratory failure. *ERJ Open Research* **9**, (2023).

- 785 11. Fair, K. *et al.* Rectal Swabs from Critically Ill Patients Provide Discordant Representations of the Gut
786 Microbiome Compared to Stool Samples. *mSphere* **4**, (2019).
- 787 12. Kitsios, G. D. *et al.* The upper and lower respiratory tract microbiome in severe aspiration pneumonia.
788 *iScience* **26**, 106832 (2023).
- 789 13. Britton, N. *et al.* Respiratory Fungal Communities are Associated with Systemic Inflammation and
790 Predict Survival in Patients with Acute Respiratory Failure. *medRxiv* (2023)
791 doi:10.1101/2023.05.11.23289861.
- 792 14. ARDS Definition Task Force *et al.* Acute respiratory distress syndrome: the Berlin Definition. *JAMA* **307**,
793 2526–2533 (2012).
- 794 15. Nguyen, L. H. *et al.* Metagenomic assessment of gut microbial communities and risk of severe COVID-
795 19. *Genome Med.* **15**, 49 (2023).
- 796 16. Zhao, J., Murray, S. & Lipuma, J. J. Modeling the impact of antibiotic exposure on human microbiota.
797 *Sci. Rep.* **4**, 4345 (2014).
- 798 17. Wang, A. A. *et al.* The Narrow-Spectrum Antibiotic Treatment Score: A Novel Quantitative Tool for
799 Assessing Broad- and Narrow-Spectrum Antibiotic Use in Severe Community-Acquired Pneumonia. in
800 *B28. HOST AND MICROBIAL CLINICAL STUDIES IN LUNG INFECTIONS AND LUNG DISEASES*
801 *A2929–A2929* (American Thoracic Society, 2020). doi:10.1164/ajrccm-
802 conference.2020.201.1_MeetingAbstracts.A2929.
- 803 18. Holmes, I., Harris, K. & Quince, C. Dirichlet multinomial mixtures: generative models for microbial
804 metagenomics. *PLoS ONE* **7**, e30126 (2012).
- 805 19. Narayana, J. K., Mac Aogáin, M., Ali, N. A. B. M., Tsaneva-Atanasova, K. & Chotirmall, S. H. Similarity
806 network fusion for the integration of multi-omics and microbiomes in respiratory disease. *Eur. Respir. J.*
807 **58**, (2021).

- 808 20. Drohan, C. M. *et al.* Biomarker-Based Classification of Patients With Acute Respiratory Failure Into
809 Inflammatory Subphenotypes: A Single-Center Exploratory Study. *Crit. Care Explor.* **3**, e0518 (2021).
- 810 21. Kitsios, G. D., Franz, C. & McVerry, v. The Microbiome in Acute Lung Injury and ARDS. in *The*
811 *Microbiome in Respiratory Disease* (eds. Huang, Y. J. & Garantziotis, S.) (Humana, Cham, 2022).
- 812 22. Lloréns-Rico, V. *et al.* Clinical practices underlie COVID-19 patient respiratory microbiome composition
813 and its interactions with the host. *Nat. Commun.* **12**, 6243 (2021).
- 814 23. Bernard-Raichon, L. *et al.* Gut microbiome dysbiosis in antibiotic-treated COVID-19 patients is
815 associated with microbial translocation and bacteremia. *Nat. Commun.* **13**, 5926 (2022).
- 816 24. Chanderraj, R. *et al.* In critically ill patients, anti-anaerobic antibiotics increase risk of adverse clinical
817 outcomes. *Eur. Respir. J.* (2022) doi:10.1183/13993003.00910-2022.
- 818 25. Pickens, C. O. *et al.* Bacterial Superinfection Pneumonia in Patients Mechanically Ventilated for
819 COVID-19 Pneumonia. *Am. J. Respir. Crit. Care Med.* **204**, 921–932 (2021).
- 820 26. Kullberg, R. F. J., Schinkel, M. & Wiersinga, W. J. Empiric anti-anaerobic antibiotics are associated with
821 adverse clinical outcomes in emergency department patients. *Eur. Respir. J.* **61**, (2023).
- 822 27. Kitsios, G. D. & McVerry, B. J. Host-Microbiome Interactions in the Subglottic Space. *Bacteria Ante*
823 *Portas!* *Am. J. Respir. Crit. Care Med.* **198**, 294–297 (2018).
- 824 28. Dickson, R. P. *et al.* Bacterial topography of the healthy human lower respiratory tract. *MBio* **8**, (2017).
- 825 29. Zhao, T. *et al.* Oral hygiene care for critically ill patients to prevent ventilator-associated pneumonia.
826 *Cochrane Database Syst. Rev.* **12**, CD008367 (2020).
- 827 30. Hammond, N. E. *et al.* Association Between Selective Decontamination of the Digestive Tract and In-
828 Hospital Mortality in Intensive Care Unit Patients Receiving Mechanical Ventilation: A Systematic
829 Review and Meta-analysis. *JAMA* **328**, 1922–1934 (2022).

- 830 31. Klompas, M. Oropharyngeal Decontamination with Antiseptics to Prevent Ventilator-Associated
831 Pneumonia: Rethinking the Benefits of Chlorhexidine. *Semin. Respir. Crit. Care Med.* **38**, 381–390
832 (2017).
- 833 32. Buelow, E. *et al.* Comparative gut microbiota and resistome profiling of intensive care patients receiving
834 selective digestive tract decontamination and healthy subjects. *Microbiome* **5**, 88 (2017).
- 835 33. Horn, K. J., Schopper, M. A., Drigot, Z. G. & Clark, S. E. Airway Prevotella promote TLR2-dependent
836 neutrophil activation and rapid clearance of *Streptococcus pneumoniae* from the lung. *Nat. Commun.*
837 **13**, 3321 (2022).
- 838 34. Segal, L. N. *et al.* Enrichment of lung microbiome with supraglottic taxa is associated with increased
839 pulmonary inflammation. *Microbiome* **1**, 19 (2013).
- 840 35. Wu, B. G. *et al.* Episodic Aspiration with Oral Commensals Induces a MyD88-dependent, Pulmonary T-
841 Helper Cell Type 17 Response that Mitigates Susceptibility to *Streptococcus pneumoniae*. *Am. J.*
842 *Respir. Crit. Care Med.* **203**, 1099–1111 (2021).
- 843 36. Dickson, R. P. *et al.* Enrichment of the lung microbiome with gut bacteria in sepsis and the acute
844 respiratory distress syndrome. *Nat. Microbiol.* **1**, 16113 (2016).
- 845 37. Nath, S., Kitsios, G. D. & Bos, L. D. J. Gut-lung crosstalk during critical illness. *Curr. Opin. Crit. Care*
846 **29**, 130–137 (2023).
- 847 38. Bain, W. *et al.* Research Bronchoscopy Standards and the Need for Non-Invasive Sampling of the
848 Failing Lungs. *Ann Am Thorac Soc* (2023).
- 849 39. Shankar-Hari, M., Fan, E. & Ferguson, N. D. Acute respiratory distress syndrome (ARDS) phenotyping.
850 *Intensive Care Med.* **45**, 516–519 (2019).
- 851 40. Kalil, A. C. *et al.* Management of Adults With Hospital-acquired and Ventilator-associated Pneumonia:
852 2016 Clinical Practice Guidelines by the Infectious Diseases Society of America and the American
853 Thoracic Society. *Clin. Infect. Dis.* **63**, e61–e111 (2016).

- 854 41. Morris, A. *et al.* Comparison of the respiratory microbiome in healthy nonsmokers and smokers. *Am. J.*
855 *Respir. Crit. Care Med.* **187**, 1067–1075 (2013).
- 856 42. Kitsios, G. D. *et al.* Respiratory microbiome profiling for etiologic diagnosis of pneumonia in
857 mechanically ventilated patients. *Front. Microbiol.* **9**, 1413 (2018).
- 858 43. Charalampous, T. *et al.* Nanopore metagenomics enables rapid clinical diagnosis of bacterial lower
859 respiratory infection. *Nat. Biotechnol.* **37**, 783–792 (2019).
- 860 44. Yang, L. *et al.* Metagenomic identification of severe pneumonia pathogens in mechanically-ventilated
861 patients: a feasibility and clinical validity study. *Respir. Res.* **20**, 265 (2019).
- 862 45. Juul, S. *et al.* What's in my pot? Real-time species identification on the MinION. *BioRxiv* (2015)
863 doi:10.1101/030742.
- 864 46. Huber, W. *et al.* Orchestrating high-throughput genomic analysis with Bioconductor. *Nat. Methods* **12**,
865 115–121 (2015).
- 866 47. R Foundation for Statistical Computing, R. C. T. *R: A Language and Environment for*
867 *Statistical Computing*. (CRAN, 2016).
- 868 48. Raghu, V. K. *et al.* Comparison of strategies for scalable causal discovery of latent variable models
869 from mixed data. *Int. J. Data Sci. Anal.* **6**, 33–45 (2018).

Supplementary Files

This is a list of supplementary files associated with this preprint. Click to download.

- [SupplementKitsiosMultiComp9.8.23.pdf](#)